

# Auto-calibration and -compensation of a capacitive pressure sensor using multilayer perceptrons

*Jagdish C. Patra<sup>abc</sup>, Adriaan van den Bos<sup>c</sup>*

*<sup>a</sup>Nanyang Technological University, School of Electrical and Electronic Engineering, Block S2-B3a-06, Nanyang Avenue, 639798, Singapore. Tel.: +65- 790-5369 ext. 6298; fax: +65-792-0415/793-3318.*

*<sup>b</sup>On leave from the Department of Applied Electronics & Instrumentation Engineering, Regional Engineering College, Rourkela, Orissa 769 008, India.*

*<sup>c</sup>Department of Applied Physics, Delft University of Technology, PO Box 5046, 2600 GA Delft, The Netherlands; E-mail addresses: [ejcpatra@ntu.edu.sg](mailto:ejcpatra@ntu.edu.sg), [jcpatra@hotmail.com](mailto:jcpatra@hotmail.com) (J.C. Patra), [a.vandenbos@tn.tudelft.nl](mailto:a.vandenbos@tn.tudelft.nl) (A. van den Bos).*

## Abstract

Using multilayer perceptrons (MLPs), a smart model for a capacitive pressure sensor (CPS) is proposed. When the ambient temperature changes, the nonlinear response characteristics of a CPS may vary widely. Under such conditions, calibration of the sensor and compensation of the nonlinear sensor characteristics to obtain correct readout becomes a difficult task. The proposed MLP model can provide automatic nonlinear compensation and calibration of the CPS characteristics. A microcontroller unit (MCU)-based implementation scheme for this model is also considered. Simulation results show that this model can estimate the pressure with a maximum full-scale error of  $\pm 1\%$  over a variation of temperature from  $-50$  to  $150$  °C.

*Keywords:* Auto-calibration; Smart pressure sensor; Multilayer perceptron

## 1. Introduction

In various autonomous industries, capacitive pressure sensors (CPSs) are being widely applied because they have a higher sensitivity and lower power dissipation than other pressure sensors. However, some of the difficulties associated with the CPS are: (i) its response characteristics are highly nonlinear, (ii) its change in capacitance is small compared to the offset capacitance, and (iii) its response characteristics change substantially when the variation of operating temperature is large. Therefore, in a dynamic environment in which the ambient temperature undergoes a large variation, the CPS needs appropriate compensation to mitigate the adverse effects of the temperature besides corrections to its nonlinear characteristics.

Sensor calibration contributes considerably to the sensor price. Often, the cost of calibration far exceeds the primary manufacturing costs. To minimize the number of measurements required for calibration, a sensor model must be chosen to which the actual curve fits. Under harsh operating conditions, such

as oil, gas wells and chemical and nuclear industries, where human intervention is not possible, there is a need of auto-calibration and compensation of the sensor characteristics to obtain the correct pressure readout [1,2].

Under such conditions, several signal processing techniques have been proposed for a CPS to obtain the correct readout of the applied pressure [3–5]. These techniques include both iterative and non-iterative algorithms, and involve complex signal processing for the modeling of the CPS. They offer satisfactory performance unless the temperature variation is large.

<b>Nomenclature</b>	
A/D	analogue to digital
ADC	analogue to digital converter
ANN	artificial neural network
BP	backpropagation
CPS	capacitive pressure sensor
EPROM	electrically programmable read only memory
FS	full scale
MCU	micro-controller unit
MLP	multilayer perceptron
RAM	random access memory
ROM	read only memory
SCI	switched capacitor interface
SF	scale factor

Recently, artificial neural networks (ANNs) have emerged as a powerful learning technique to perform complex tasks in highly nonlinear dynamic environments. These networks are endowed with certain unique characteristics: the capability of universal approximation, the ability to learn from and to adapt to their environment, and the ability to cope with weak assumptions about the underlying physical phenomenon responsible for generation of input data. Another important property of the ANNs is their fault tolerance capability; because of which graceful degradation of performance takes place if the network is partially damaged. Because of these characteristics, there have been numerous successful applications of ANNs in various fields of science, engineering and industry [6] including instrumentation and measurement [7,8] in general, and CPSs in particular [9–13].

In [9], a simple functional link ANN (FLANN) has been employed to estimate the nonlinearity and for direct digital readout of a CPS. The response characteristics of the CPS was modeled in terms of a power series. The FLANN was used to accurately estimate the coefficients of the series.

From the knowledge of these coefficients, the nonlinearity of the CPS can be estimated and the applied pressure readout can be obtained. The multilayer perceptron (MLP) is the most popularly used ANN in many applications. A smart pressure sensor using an MLP has been reported [10]. This model can provide an accurate pressure readout when the ambient temperature changes from  $-20$  to  $70$  °C. The computational complexity of a model plays an important role for implementation purposes. A computationally efficient ANN has been proposed for modeling of a CPS in [11]. This model requires less number computations than an MLP-based model for implementation. It provides an accurate estimate of the applied pressure over a wide variation of ambient temperature from  $-50$  to  $150$  °C with a full scale (FS) percentage error of  $\pm 1\%$ .

In [10] and [11], it was assumed that the CPS response characteristics change linearly with temperature. However, in practice, the influence of ambient temperature on the CPS characteristics is nonlinear in nature. This aspect was studied using a MLP-based CPS model and its performance has been reported in [12]. It has been shown that, in a dynamic environment in which nonlinear interaction of temperature on the sensor characteristics takes place, the MLP-based model can provide an accurate estimate of the applied pressure over a wide variation of temperatures from  $-50$  to  $150$  °C with a FS percentage error of  $\pm 3\%$ . An MLP-based compensation scheme for systematic uncertainties of the sensors subject to combined influence parameters using a second sensor has been proposed [13].

In the present paper, we propose a smart MLP-based model of a CPS to provide auto-calibration and auto-compensation of the nonlinear and temperature dependent sensor characteristics. The proposed modeling approach is radically different from those of Refs. [9–12]. In these papers, the ANNs have been used to track the sensor characteristics at different temperatures. The ANN learns the sensor characteristics for the given range of temperature. With the knowledge of the ambient temperature and the capacitance change, the ANN model provides an accurate readout of the applied pressure. With the assumption that the sensor characteristics at different temperatures provide the correct response, these ANN models can track the response characteristics accurately and give a correct pressure readout.

In the present paper, on the other hand, the pressure readout is carried out by using two MLPs. The first MLP is utilized to transfer the sensor characteristics at any value of temperature to the normalized calibrated sensor characteristics. The second MLP is used to estimate the applied pressure from the knowledge of capacitance change in the sensor. In this approach, calibration and compensation of the sensor characteristics can be made automatically. The first MLP provides the calibrated response characteristics irrespective of change in the sensor characteristics due to change in ambient temperature. The second MLP compensates the nonlinearity in the response characteristics and provides accurate pressure readout. Through extensive simulation studies, it is shown

that the proposed MLP-based model provides a maximum FS error of  $\pm 1\%$  in estimation of pressure for temperature variations from  $-50$  to  $150$  °C. A microcontroller unit (MCU)-based scheme for implementation of the CPS model is also suggested.

## 2. Capacitive pressure sensor and switched capacitor interface

A CPS senses the applied pressure in the form of elastic deflection of its diaphragm. The normalized capacitance of a CPS resulting from the applied pressure  $P$  at the ambient temperature  $T$  is given by:

$$C_N = C(P, T)/C_0 \quad (1)$$

where

$$\begin{aligned} C(P, T) &= C_0(T) + \Delta C(P, T), \\ &= C_0 f_1(T) + \Delta C(P, T_0) f_2(T). \end{aligned} \quad (2)$$

The offset capacitance at the reference temperature  $T_0$  is denoted by  $C_0$ . When pressure is applied to the CPS, its change in capacitance at the reference temperature is given by:

$$\Delta C(P, T_0) = C_0 P_N \frac{1 - \tau}{1 - P_N}, \quad (3)$$

where  $\tau$  is the sensitivity parameter of the CPS which depends on its geometrical structure,  $P_N$  is the normalized applied pressure given by  $P_N = P/P_{max}$ , and  $P_{max}$  is the maximum permissible applied pressure. We assume that the change in capacitance as function of temperature is linear. The linear functions are  $f_i(T)$ ,  $i = 1, 2$ , and are described by:

$$f_i(T) = 1 + g_i(T), \quad (4)$$

where

$$g_i(T) = \eta_i T_n, \quad (5)$$

$T_n = \frac{T - T_0}{T_{max}}$  and  $\eta_i$ ,  $i = 1, 2$  are the coefficients which determine the influence of the temperature on the sensor characteristics.

It follows from Eq. (1) that

$$C_N = f_1(T) + \gamma f_2(T), \quad (6)$$

where  $\gamma = P_N(1 - \tau)/(1 - P_N)$ . Because of requirement of the ANN modeling, the  $C_N$  in Eq. (6) is divided by a factor of 2, so as to keep its maximum value within 1. The normalized temperature  $T_N$  is defined as  $T_N = T/T_{max}$ , where  $T_{max}$  is the maximum permissible temperature at which the sensor may be operated.

If the applied pressure is zero, then  $\gamma$  becomes zero. Therefore, the normalized capacitance at zero applied pressure is given by:

$$C_{N0} = f_1(T) = 1 + g_1(T). \quad (7)$$

A switched capacitor interface (SCI) for the CPS is shown in Fig. 1. The CPS is represented by  $C(P)$ . The SCI output provides a voltage signal proportional to the capacitance change in the CPS due to applied pressure. The SCI operation can be controlled by a reset signal  $\theta$ . When  $\bar{\theta} = 1$  (logic 1),  $C(P)$  charges to the reference voltage  $V_R$  while the capacitor  $C_S$  is discharged to ground. Whereas, when  $\theta = 1$ , the total charge  $C(P)V_R$  stored in the  $C(P)$  is transferred to  $C_S$  producing an output voltage given by:

$$V_O = K \cdot C(P), \quad (8)$$

where  $K = -V_R/C_S$ . It may be noted that if the ambient temperature changes, then the SCI output also changes, although the applied pressure remains the same. By choosing proper values of  $C_S$  and  $V_R$  the normalized SCI output  $V_N$  may be obtained in such a way that

$$V_N = C_N \quad (9)$$

The unnormalized and normalized SCI output for zero applied pressure are denoted by  $V_{00}$  and  $V_{N0}$ , respectively. Therefore, if  $P_N = 0$ , then  $V_{N0} = C_{N0}$ . From Eq. (7) it may be seen that from the measurement of  $C_{N0}$ , or  $V_{N0}$ , one can obtain the temperature information. Therefore, instead of using some other source (perhaps a temperature sensor) for obtaining temperature information, the same can be obtained from the measurement of  $C_{N0}$ , i.e. from the CPS characteristics itself. In our proposed model, we have used  $V_{N0}$  to get the value of the temperature. The normalized calibrated pressure and capacitance are denoted by  $P_{NC}$  and  $C_{NC}$ , respectively.

### 3. The multilayer perceptron and backpropagation algorithm

The multilayer perceptron is a feedforward network in which there may be one or more hidden layers besides one input and one output layer. Each layer may contain one or more nonlinear processing unit called a 'neuron', or 'node'. All layers except the output layer contain a bias or threshold node whose output is set to a fixed value of 1. All the nodes of a lower layer are connected to all the nodes of an upper layer through links called weights. The backpropagation (BP) algorithm, a generalized steepest descent algorithm, is the most popular learning technique used to train the MLP. The weights of the MLP are updated by using the BP algorithm during the training phase. The

knowledge acquired by the network after learning is stored in its weights in a distributed manner. The MLP and the BP algorithm are briefly discussed below. For the details one may refer to Ref. [6].

Consider an  $L$ -layer MLP as shown in Fig. 2. In this network, the number of nodes (excluding the threshold unit) in the input and output layers are  $N_0$  and  $N_L$ , respectively. The number of nodes (excluding the threshold unit) in the hidden layers is denoted by  $N_l$  where  $l = 1, 2, \dots, L - 1$ . The architecture of an  $L$ -layer MLP is denoted by  $\{N_0 - N_1 - \dots - N_L\}$ . During training phase, an input pattern, and its corresponding desired or target pattern is applied to the network. At the  $k$ th instant let the input pattern applied to the MLP be denoted by  $\{u_i(k)\}$ , where  $i = 1, 2, \dots, N_0$ . No computation takes place in the input layer of the MLP and hence, the node output for this layer is given by  $x_i^{(0)} = u_i(k)$ . The node outputs for other layers at the  $k$ th instant are given by:

$$x_i^{(l)} = \rho(S_i^{(l)}) \quad (10)$$

for  $l = 1, 2, \dots, L$ , and  $i = 1, 2, \dots, N_l$ , where,

$$S_i^{(l)} = \sum_{j=0}^{N_{l-1}} x_j^{(l-1)} w_{ij}^{(l)}, \quad (11)$$

$x_i^{(l-1)}$  is the  $i$ th node output of the  $(l - 1)$ th layer,  $w_{ij}^{(l)}$  is the connection weight from the  $j$ th node of  $(l - 1)$ th layer to  $i$ th layer of  $l$ th layer, and  $x_0^{(l-1)}$  is the bias unit whose output is set to 1. The most popular nonlinear function  $\rho(\cdot)$  is given by

$$\rho(z) = \tanh(z) = \frac{1 - \exp(-2z)}{1 + \exp(-2z)}. \quad (12)$$

This function provides an output ranging from  $-1.0$  to  $1.0$ , and this range of output is quite helpful in solving many practical problems.

Let the output of the MLP, and the target output at the  $k$ th instant be represented by  $\{y_i(k)\}$  and  $\{d_i(k)\}$ , where  $i = 1, 2, \dots, N_L$ , respectively. Then,  $y_i(k) = x_i^{(L)}$ . The error at the  $k$ th instant is given by

$$e_i(k) = d_i(k) - y_i(k). \quad (13)$$

Thus, the sum of square errors produced by the MLP is given by

$$E(k) = \sum_{i=1}^{N_L} [e_i(k)]^2. \quad (14)$$

The BP algorithm attempts to minimize the cost function  $E(k)$  recursively by updating

the weights of the network.

The algorithm for weight update at the  $k$ th instant is given by Ref. [6]:

$$w_{ij}^{(l)}(k+1) = w_{ij}^{(l)}(k) + \alpha \Delta_{ij}(k) + \beta \Delta_{ij}(k-1), \quad (15)$$

where

$$\Delta_{ij}(k) = \delta_i^{(l)} x_j^{(l-1)} \text{ for } l = L, L-1, \dots, 1, \quad (16)$$

$$\delta_i^{(l)} = e_i(k) \rho'(S_i^{(l)}) \text{ for } l = L, \quad (17)$$

$$\delta_i^{(l)} = \left( \sum_{j=1}^{N_{l+1}} \delta_j^{(l+1)} w_{ji}^{(l+1)}(k) \right) \rho'(S_i^{(l)}) \text{ for } \quad (18)$$

$$l = L-1, L-2, \dots, 1,$$

and  $S_i^{(l)}$  is defined in Eq. (11). The BP algorithm is a generalized form of steepest descent algorithm which attempts to find optimum weights to minimize the chosen cost function. The partial derivative of the hyperbolic tangent function with respect to  $S$  is denoted by  $\rho'(S)$ . The so-called learning rate and the momentum rate are denoted by  $\alpha$  and  $\beta$ , respectively, and their values should lie between 0 and 1.

#### 4. The MLP-based CPS model

In certain systems, such as missiles, aircrafts, and chemical and process industries, the CPS may be operated in a dynamic environment in which the temperature variation may be quite large. To cope with these conditions, to obtain correct pressure readout, we propose a model using two MLPs to take care of variation of temperature from  $-50$  to  $150^\circ\text{C}$ .

The proposed MLP-based model for auto-calibration and -compensation uses two MLPs. The first MLP is used to transfer the sensor characteristics at any temperature to the calibrated normalized sensor characteristics. When the ambient temperature changes, the sensor characteristics also change. However, the MLP has been trained to produce the calibrated characteristics irrespective of variation in ambient temperature. Therefore, at any ambient temperature, the first MLP model provides the calibrated sensor response characteristics. The second MLP is used to compensate the nonlinearity in the response characteristics, and to estimate the applied pressure.

In this MLP-based CPS model, all the signals used are suitably scaled by appropriate scale factors (SFs) to keep their range within  $\pm 1.0$ . The model operates in two phases: the training phase and the test phase. In the training phase, the ANNs used in the model are trained to learn the sensor characteristics and the environment. Several data-sets are

needed to train the MLPs. An input pattern, and its corresponding desired, or target pattern constitute one pair of data in the data-set. The available data-sets are segregated into two parts. The first part, called training-set, is used for training of the ANNs, and the other part called test-set, is used for testing the model to verify its effectiveness.

During the training phase, an input pattern from the training-set is applied to the ANN. Then, the output of the ANN is computed. This output is compared with the corresponding target pattern. The error obtained from this comparison is then used to update the weights of the MLP using the BP algorithm described in Section 3. This training procedure continues till the error reaches a preset minimum value. Next, the final weights are stored in an EPROM to be used during testing and actual use of the sensor model.

During the second phase, i.e. the test phase, the stored final weights are loaded into the MLPs. An input pattern from the test-set is applied to the ANN model and its output is computed. If the ANN output and the target pattern match closely, then it may be said that the ANN model has learned the sensor characteristics satisfactorily.

#### *4.1. Transfer of sensor characteristics*

In the first stage, the MLP-1 is trained to learn to transfer the sensor characteristics at any temperature to the normalized calibrated response characteristics. The scheme for this is shown in Fig. 3. Here, the inputs to the MLP-1 consist of the normalized temperature ( $T_N$ ), and normalized SCI output ( $V_N$ ). The desired (or the target) output for the MLP is the normalized calibrated capacitance ( $C_{NC}$ ). The MLP output provides an estimate of the normalized calibrated capacitance,  $\hat{C}_{NC}$ . One data-set for a specific temperature is obtained by recording the SCI output ( $V_N$ ) for different values of applied pressure, covering the operating range of the sensor at that temperature. Next, at different temperature values, covering the full operating range, data-sets are generated. The MLP-1 is trained by taking the patterns from the training-set, and its weights are updated by using the BP algorithm. After training, the weights of the MLP are frozen and stored in an EPROM. In what follows, these final weights are denoted by  $W_1$ .

#### *4.2. Estimation of pressure*

The scheme of estimation of the pressure and compensation to the nonlinear response characteristics is shown in Fig. 4. Here, the input to the MLP-2 is the normalized capacitance, and the target output is the normalized calibrated pressure. The output of the MLP provides the estimate of the normalized pressure. The error between the MLP output and the target output is used to update the weights of the MLP by the BP algorithm. After the training is complete, the final weights are stored in an EPROM. In what follows, these final weights are denoted by  $W_2$ .

#### *4.3. Test phase and the complete model*

The complete scheme of the MLP-based model is shown in Fig. 5. This model can provide the calibrated pressure readout accurately independent of variation of temperature and nonlinear response characteristics. During test-phase, and actual use, the weights  $W_1$  and  $W_2$ , stored in the EPROM are loaded into the MLP-1 and MLP-2, respectively. The MLP-1 has learned to transfer the CPS response characteristics at any temperature to the normalized calibrated characteristics. The MLP-2 has learned the nonlinear calibrated response characteristics and to estimate the pressure. The input patterns from the test-set are applied, and the model output ( $\hat{P}_{NC}$ ) is computed. If the model output matches the actual applied pressure ( $P_N$ ) closely, then it may be said that the MLPs have learned the CPS characteristics correctly. Then, the model can be used in practice to estimate the pressure and to obtain pressure readout.

## 5. Simulation studies

We have carried out extensive simulation studies to evaluate the performance of the proposed MLP-based CPS model. In the following we describe the details of the simulation study.

### 5.1. Preparation of data-sets

All the parameters of the CPS, such as, ambient temperature, applied pressure, and the SCI output voltage, used in the simulation study were suitably normalized so as to keep their values within  $\pm 1.0$ . Appropriate SFs were chosen for this purpose. Several data-sets are needed for training as well as for testing of the MLP model. These data-sets are generated as follows. The SCI voltage ( $V_N$ ) was recorded [see Eq. (9)] at the reference temperature (25 °C) at different known values of normalized pressure ( $P_N$ ) chosen between 0.0 and 0.6 at an interval of 0.05. Thus, these 13 pairs of data ( $P_N$  and  $V_N$ ) constitute one data-set at the reference temperature.

We have chosen the values of  $\eta_1$  and  $\eta_2$  as  $-2 \times 10^{-3}$  and  $7 \times 10^{-3}$ , respectively. With the knowledge of the data-set at reference temperature, and the chosen values of  $\eta_i$ , and using Eq. (6), the response characteristics of the CPS for a specific ambient temperature were generated. Each of these response characteristics consists of 13 pairs of data ( $P_N$  and  $V_N$ ), and corresponds to a data-set at that temperature. For a temperature range from  $-50$  to  $150$  °C, at an increment of  $10$  °C, 21 data-sets, each containing 13 data pairs were generated. Next, these data-sets were divided into two groups: the training-set and the test-set. The training-set, used for training of the MLPs, consists of 5 data-sets corresponding to  $-50$ ,  $0$ ,  $50$ ,  $100$  and  $150$  °C, and the remaining 16 data-sets constitute the test-set.

The response characteristics of the CPS at different values of temperature, and the calibrated response are shown in Fig. 6. It may be observed that wide variation in the sensor characteristics occurs when the ambient temperature changes from  $-50$  to  $150$  °C.

### 5.2. Training and testing of MLP-1

In Fig. 3, a 2-layer MLP with {2-5-1} architecture was chosen for MLP-1 in this modeling problem. The two inputs to the MLP were the normalized temperature ( $T_N$ ), and the normalized SCI output voltage ( $V_N$ ). The target output for the MLP was the calibrated normalized capacitance ( $C_{NC}$ ).

Initially, all the weights of the MLP-1 were set to some random values within  $\pm 0.5$ . During training, the five data-sets were chosen randomly. Also, the individual patterns of each set were selected in a random manner. After application of one input pattern, the MLP-1 produces an output  $\hat{C}_{NC}$ , which was compared with the target pattern to obtain an error value. This error was used to update the weights of the MLP using the BP algorithm discussed in Section 3. For both, the learning parameter  $\alpha$ , and the momentum factor  $\beta$ , of Eq. (15), the value was chosen as 0.75. Next, another pattern was applied, and this process continues till the mean square error between the target and the MLP output reaches a minimum value. Completion of weight adaptation for the 13 data pairs of all the five training-sets constitutes one iteration. For effective learning, 30,000 iterations were made to train the MLP model. At the end, the final weights of the MLP-1 ( $W_1$ ) were stored for later use for performance evaluation and actual use of the model. The final weights of the MLP-1 are provided in Table 1.

The performance evaluation of the MLP-1 was carried out by loading the final stored weights into the MLP. It may be noted that, during testing, and actual use of the CPS model, there is no updating of the weights. The inputs are applied to the model, and the MLP estimates the applied pressure from the knowledge of the stored weights loaded into it. For testing purposes, the SCI output voltage was simulated with a range from 0.35 to 0.80 with an increment of 0.001, and then applied to the MLP along with the temperature information. To evaluate the effectiveness of the model, the MLP output ( $\hat{C}_{NC}$ ) was computed and then compared with the true values of normalized calibrated capacitance ( $C_{NC}$ ).

### 5.3. Training and testing of MLP-2

The MLP-2 is used to compensate the non-linearity of the response characteristics and to estimate the calibrated pressure readout (see Fig. 4). The input to the MLP are the values of calibrated normalized capacitance ( $C_{NC}$ ) and the target output is the normalized calibrated pressure ( $P_N$ ). The MLP output produces the estimated calibrated pressure ( $\hat{P}_N$ ).

An MLP with {1-4-1} architecture was chosen for this purpose. The 13 pairs of data patterns corresponding to the calibration points are used to train the MLP. After application of the input and the corresponding target output to the MLP, its weights were updated using the BP algorithm. Both the values of  $\alpha$  and  $\beta$  were chosen as 0.8. The updating of the weights was continued up to 50,000 iterations. The final weights,  $W_2$  are tabulated in Table 2.

The testing of the MLP-2 was carried out after loading the stored weights into the network. The value of  $C_{NC}$  was varied from 0.5 to 0.85 with an increment of 0.001 and fed to the MLP. The output of the MLP and the calibrated normalized pressure were compared to verify the performance of the model.

#### *5.4. The complete model*

Fig. 5 depicts the complete model of the sensor for auto-calibration and nonlinearity compensation. When pressure is applied, the SCI converts the change in capacitance in the CPS into a corresponding voltage  $V_O$ . The temperature information is obtained from the SCI output at zero applied pressure. The stored weights are loaded into the respective MLPs. The normalized temperature and the SCI output are applied to the MLP-1. The MLP-1 estimates the calibrated capacitance. This value is fed to the MLP-2, and the MLP-2 provides an estimate of the calibrated pressure. The pressure readout can be obtained after passing the MLP-2 output through a suitable scale factor. The estimated pressure and the actual applied pressure can be compared to find the effectiveness of the model.

## **6. Results and discussions**

Here, we provide the performance results of the simulation study for auto-calibration and auto-compensation of the CPS.

### *6.1. Transfer of sensor characteristics*

The actual, calibrated and estimated (transferred) normalized capacitance at different values of temperature from the training-set are plotted in Fig. 7. Similar plots for temperature values from the test-set are shown in Fig. 8. It may be noted that the MLP-1 had not seen the sensor characteristics for the values of temperature from the test-set during the training phase. From these two figures, it may be observed that, the MLP is capable of transferring the capacitance from the actual to the calibrated values effectively over a wide range of temperature.

The FS percentage error is defined as 100 times the difference between the true or actual value and the estimated value. The FS percentage error in estimation of normalized capacitance for the temperatures from the training-set and test-set are plotted in Fig. 9. It may be seen that the FS error remains within  $\pm 1\%$  for a wide range of temperature from  $-50$  to  $150$  °C.

### *6.2. Estimation of pressure*

The calibrated pressure and estimated pressure by MLP-2 are shown in Fig. 10. The calibrated and the estimated values almost overlap each other. It may be seen from Fig. 6 that the normalized calibrated capacitance varies from 0.5 to 0.75 for the variation of normalized pressure from 0.0 to 0.6. The MLP-2 was trained with values of normalized calibrated capacitance from 0.50 to 0.75. Therefore, it is interesting to note that even for

the values of the normalized capacitance beyond 0.75, MLP-2 is capable of predicting the normalized pressure fairly well. The FS percent error in estimation of pressure is shown in Fig. 11. The MLP-2 is capable of estimating the normalized pressure with a maximum FS error of  $\pm 0.5\%$ .

### 6.3. The complete model

The actual, calibrated and estimated pressures at different values of temperature from the training-and test-sets are plotted in Fig. 12. The MLP model is capable of providing calibrated pressure readout accurately. It may be noted that both MLP-1 and MLP-2 were trained with values of  $P_N$  from 0.0 to 0.6. Therefore, it is interesting to note that even for the normalized values of pressure beyond 0.6, the model is capable of predicting the calibrated pressure fairly well. The plots of the true versus the estimated pressure at different values of temperature from the test-set, shown in Fig. 13, indicates good linearity between the two.

The FS error in estimation of pressure at different temperatures are plotted in Fig. 14. The FS percentage error at specific values of applied pressure ( $P_N = 0.1, 0.3$  and  $0.5$ ) for the whole range of temperature are shown in Fig. 15. It may be seen that the FS error remains within  $\pm 1\%$  for the whole range of temperature from  $-50$  to  $150$  °C. From the above findings, it may be concluded that the performance of the MLP model for auto-calibration and -compensation is quite effective.

## 7. An implementation scheme

Availability of low cost MCUs has led to the development of smart sensors with the capabilities of auto-calibration, self-testing, compensation and filtering of undesired signals and effects. The MCUs can be used to collect and combine data, make computations and decisions, control modes and ranges in the sensors, optimize the data rate and provide a standardized output format for higher level computer systems.

Currently available MCUs can be configured with all the required RAM/ ROM/ EPROM as well as serial interface and multiple channel A/D conversion support chips. A scheme of implementation of the MLP-based CPS model using an MCU is depicted in Fig. 16. The SCI converts the change in capacitance of the CPS due to applied pressure into an equivalent voltage level. This analogue SCI voltage is passed through an ADC. The digital temperature information is also similarly obtained from the knowledge of  $C_{N0}$ .

During the training-phase, the CPS is operated under controlled temperature and the data pairs so collected can be stored in the memories of the MCU. These training data can be fed to a PC connected to the MCU during training of the MLP-based model. After completion of training, the weights of the MLP are stored in the EPROM of the MCU. With the available hardware, such as adders and multipliers of the MCU, the MLP-based model can be implemented in the MCU. The digital readout of the applied pressure can be displayed through the data bus.

## 8. Conclusions

We have proposed an intelligent capacitive pressure sensor model using two MLPs, to compensate the nonlinear sensor characteristics, and to obtain the calibrated pressure readout. The first MLP is used to transfer the sensor characteristics at any temperature to the calibrated normalized sensor characteristics. Therefore, this model provides the calibrated response characteristics irrespective of the ambient temperature. The second MLP is used to compensate the nonlinear response characteristics and to estimate the applied pressure. The proposed approach is an improvement over earlier developments in the sense that this modeling technique calibrates the sensor characteristics automatically over a wide range of temperature variation. The proposed model can estimate the calibrated pressure with a maximum FS error of  $\pm 1\%$  for a range of temperature from  $-50$  to  $150$  °C. This model can be easily implemented using a micro-controller unit. Such MLP-based models may be applied to incorporate intelligence in other fields of instrumentation and measurement.

## References

- [1] J.H. Huijsing, F.R. Riedijk, G. van der Horn, Developments in integrated smart sensors, *Sensors and Actuators A* 43 (1994) 276–288.
- [2] G.C. Meijer, Concepts and focus points for intelligent sensor systems, *Sensors and Actuators A* 41-42 (1994) 183–191.
- [3] M. Yamada, K. Watanabe, A capacitive pressure sensor interface using oversampling  $\Delta - \Sigma$  demodulation techniques, *IEEE Transactions on Instrumentation and Measurement* 46 (1) (1997) 3–7.
- [4] K.F. Lyahou, G. van der Horn, J.H. Huijsing, A non-iterative polynomial 2-D calibration method implemented in a microcontroller, *IEEE Transactions on Instrumentation and Measurement* 46 (4) (1997) 752–757.
- [5] X. Li, G.C. Meijer, G.W. de Jong, A microcontroller-based self-calibration technique for a smart capacitance angular-position sensor, *IEEE Transactions on Instrumentation and Measurement* 46 (4) (1997) 888–892.
- [6] S. Haykin, *Neural networks*, Maxwell Macmillan, Ontario, Canada, 1994.
- [7] L.F. Pau, F.S. Johansen, Neural network signal understanding for instrumentation, *IEEE Transactions on Instrumentation and Measurement* 39 (4) (1990) 588–594.
- [8] P. Daponte, D. Grimaldi, Artificial neural networks in measurements, *Measurement* 23 (1998) 93–115.
- [9] J.C. Patra, G. Panda, R. Baliarsingh, Artificial neural network-based nonlinearity estimation of pressure sensors, *IEEE Transactions on Instrumentation and Measurement* 43 (6) (1994) 874–881.
- [10] J.C. Patra, An artificial neural network-based smart capacitive pressure sensor, *Measurement* 22 (3–4) (1997) 113–121.
- [11] J.C. Patra, A. van den Bos, Modeling of an intelligent pressure sensor using functional link artificial neural networks, *ISA Transactions*, in press.
- [12] J. C. Patra, A. van den Bos, A. C. Kot, An ANN-based smart capacitive pressure sensor in dynamic environment, *Sensors and Actuators A*.
- [13] P. Arpaia, P. Daponte, D. Grimaldi, L. Michaeli, Systematic error correction for experimentally modeled sensors by using ANNs, *Proc. IEEE IMTC'99, Venice, May 1999*, 1635–1640.

## List of Tables

- Table 1      Final weights  $W_1$  of the MLP-1 (2-5-1 architecture). First layer,  $w_{ij}$ ,  $i = 1, 2, \dots, 5$ , and  $j = 0, 1$  and  $2$ . Second layer,  $w_k$ ,  $k = 0, 1, \dots, 5$
- Table 2      Final weights  $W_2$  of the MLP-2 (1-4-1 architecture). First layer,  $w_{ij}$ ,  $i = 1, 2, \dots, 4$ , and  $j = 0, 1$  and  $2$ . Second layer,  $w_k$ ,  $k = 0, 1, \dots, 4$

## List of Figures

- Fig. 1. The switched capacitor interface circuit for a captive pressure sensor.
- Fig. 2. A multilayer perceptron structure: (a) an L-layer network ( $L = 3$ ); (b) processing in a node.
- Fig. 3. An MLP-based model of a capacitive pressure sensor for transferring the response characteristics to the calibrated characteristics.
- Fig. 4. An MLP-based model of a capacitive pressure sensor for estimation of pressure.
- Fig. 5. The complete MLP-based model of a capacitive pressure sensor.
- Fig. 6. The response characteristics of the capacitive pressure sensor at different temperatures and its calibrated (CLB) characteristics.
- Fig. 7. The actual (ACT), calibrated (CLB) and estimated (EST) response characteristics of the capacitive pressure sensor at different temperatures of training-set; (a)  $-50\text{ }^{\circ}\text{C}$ ; (b)  $0\text{ }^{\circ}\text{C}$ ; (c)  $100\text{ }^{\circ}\text{C}$ ; (d)  $150\text{ }^{\circ}\text{C}$ .
- Fig. 8. The actual (ACT), calibrated (CLB) and estimated (EST) response characteristics of the capacitive pressure sensor at different temperatures of test-set: (a)  $-20\text{ }^{\circ}\text{C}$ ; (b)  $10\text{ }^{\circ}\text{C}$ ; (c)  $80\text{ }^{\circ}\text{C}$ ; (d)  $140\text{ }^{\circ}\text{C}$ .
- Fig. 9. The full scale percentage error in estimation of calibrated capacitance by MLP-1: (a) training-set; (b) test-set.
- Fig. 10. The calibrated (CLB) and estimated (EST) pressure by MLP-2.
- Fig. 11. Full scale percentage error in estimation of pressure by MLP-2.
- Fig. 12. The calibrated (CLB), actual (ACT) and estimated (EST) pressure by the complete model at (a)  $-50\text{ }^{\circ}\text{C}$ ; (b)  $10\text{ }^{\circ}\text{C}$ ; (c)  $70\text{ }^{\circ}\text{C}$ ; (d)  $140\text{ }^{\circ}\text{C}$ .
- Fig. 13. The plots of the true versus estimated pressure at: (a)  $-30\text{ }^{\circ}\text{C}$ ; (b)  $40\text{ }^{\circ}\text{C}$ ; (c)  $90\text{ }^{\circ}\text{C}$ ; (d)  $130\text{ }^{\circ}\text{C}$ .
- Fig. 14. Full scale percentage error in estimation of pressure by the complete model at temperature values of: (a) training-set; (b) test-set.
- Fig. 15. Full scale percentage error at specific values of applied pressure ( $P_N = 0.1, 0.3$  and  $0.5$ ).
- Fig. 16. A scheme of MCU-based implementation of the model.

<i>First layer</i>		<i>i</i>				
<i>j</i>	1	2	3	4	5	
0	3.215	0.338	-0.203	-0.627	0.597	
1	1.158	0.050	2.458	-0.082	-0.727	
2	-2.930	-0.662	2.861	0.965	-1.328	
<i>Second layer</i>		<i>k</i>				
0	1	2	3	4	5	
1.339	-1.221	-0.273	0.422	0.382	-0.310	

Table 1

<i>First layer</i>		<i>i</i>			
<i>j</i>		1	2	3	4
0		1.094	0.051	1.494	-2.117
1		-1.721	-0.090	-2.200	5.419
<i>Second layer</i>		<i>k</i>			
0		1	2	3	4
-0.259		-0.295	-0.019	-0.352	0.869

Table 2

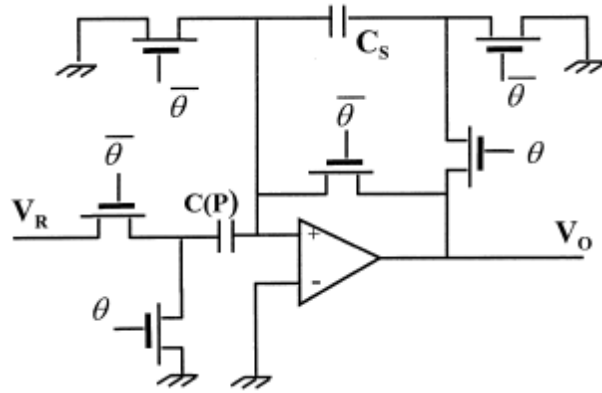


Fig. 1

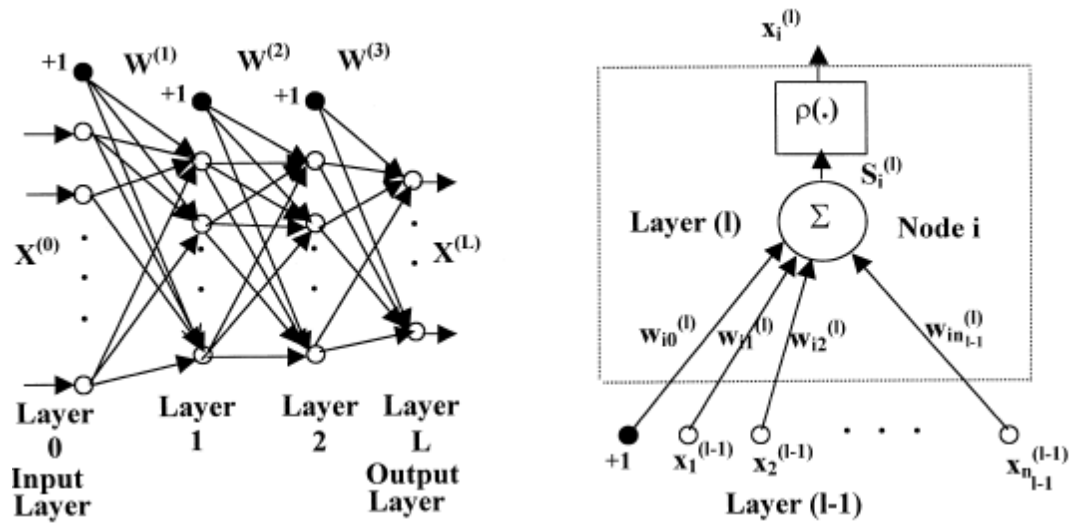


Fig. 2

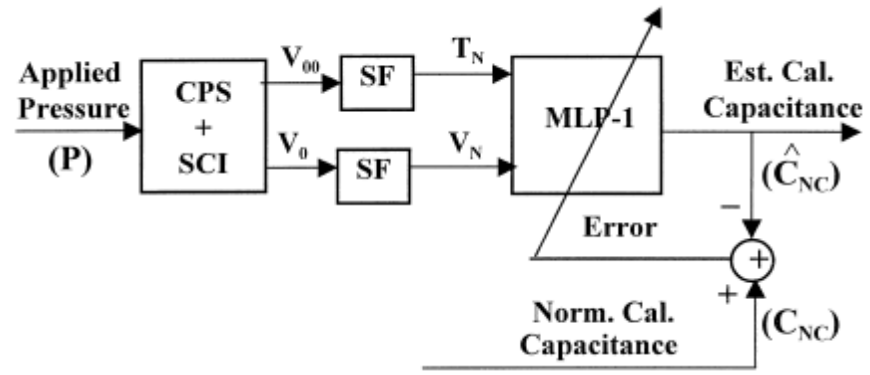


Fig. 3

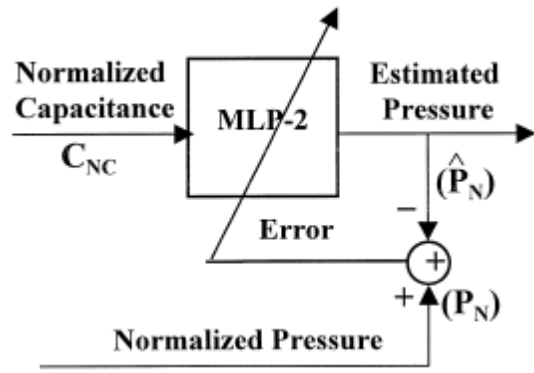


Fig. 4

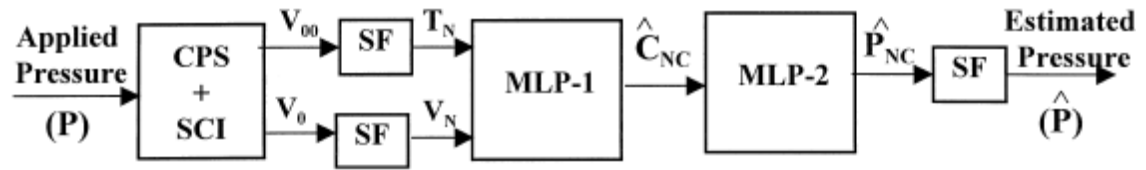


Fig. 5

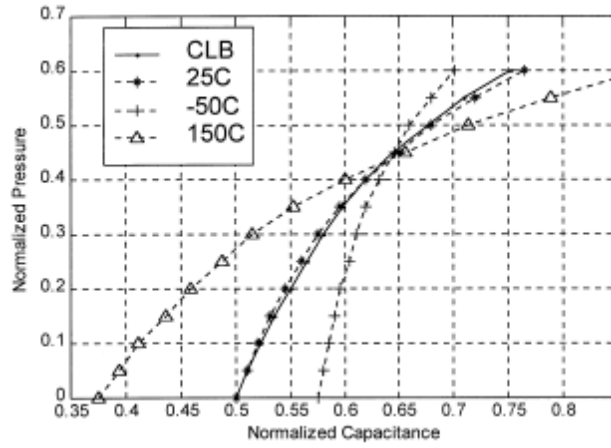


Fig. 6

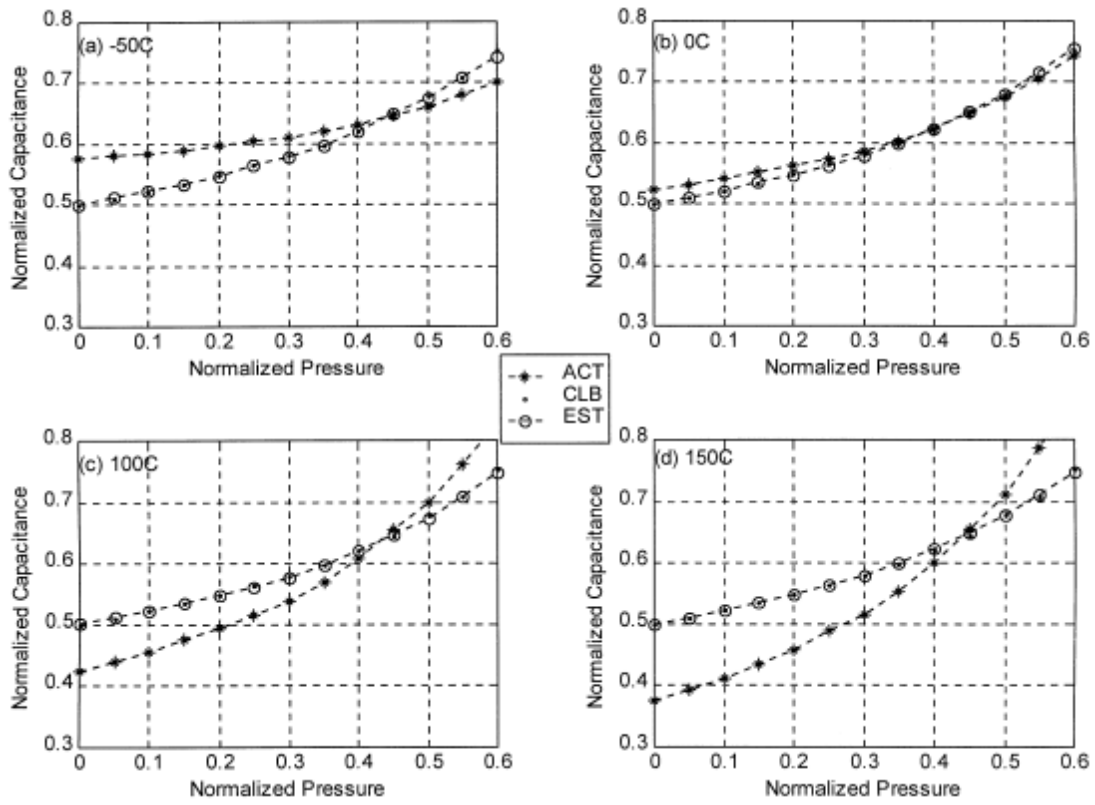


Fig. 7

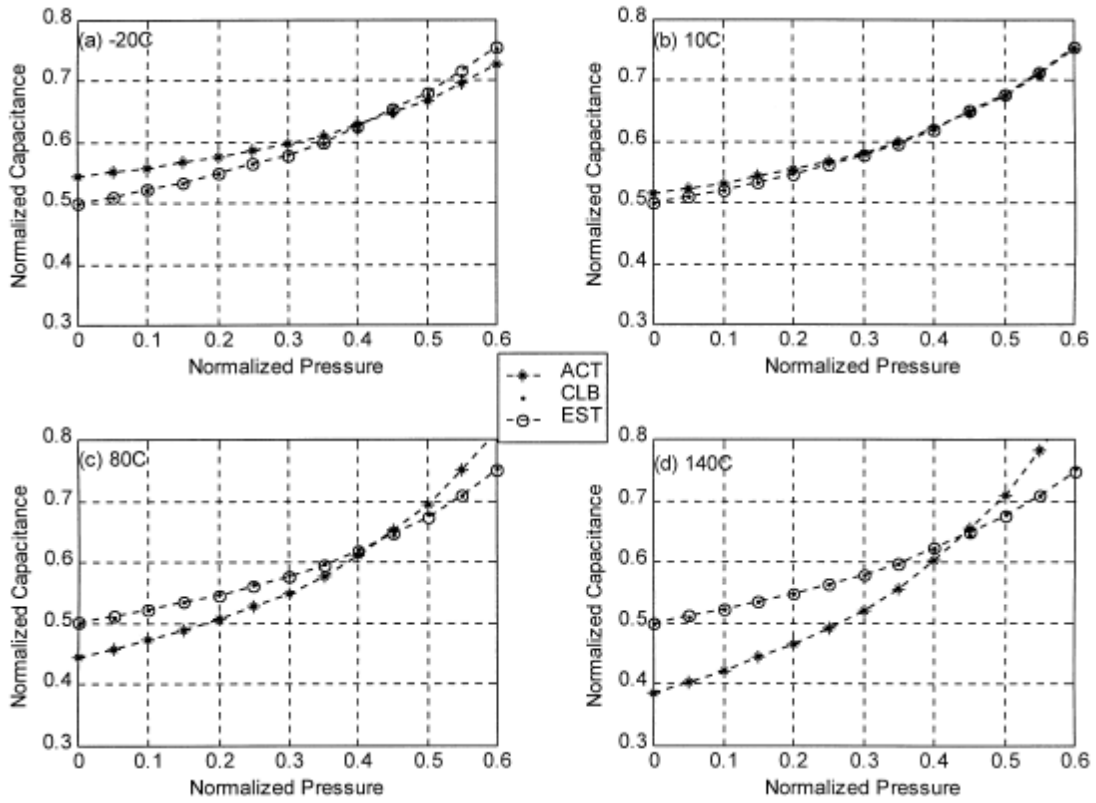


Fig. 8

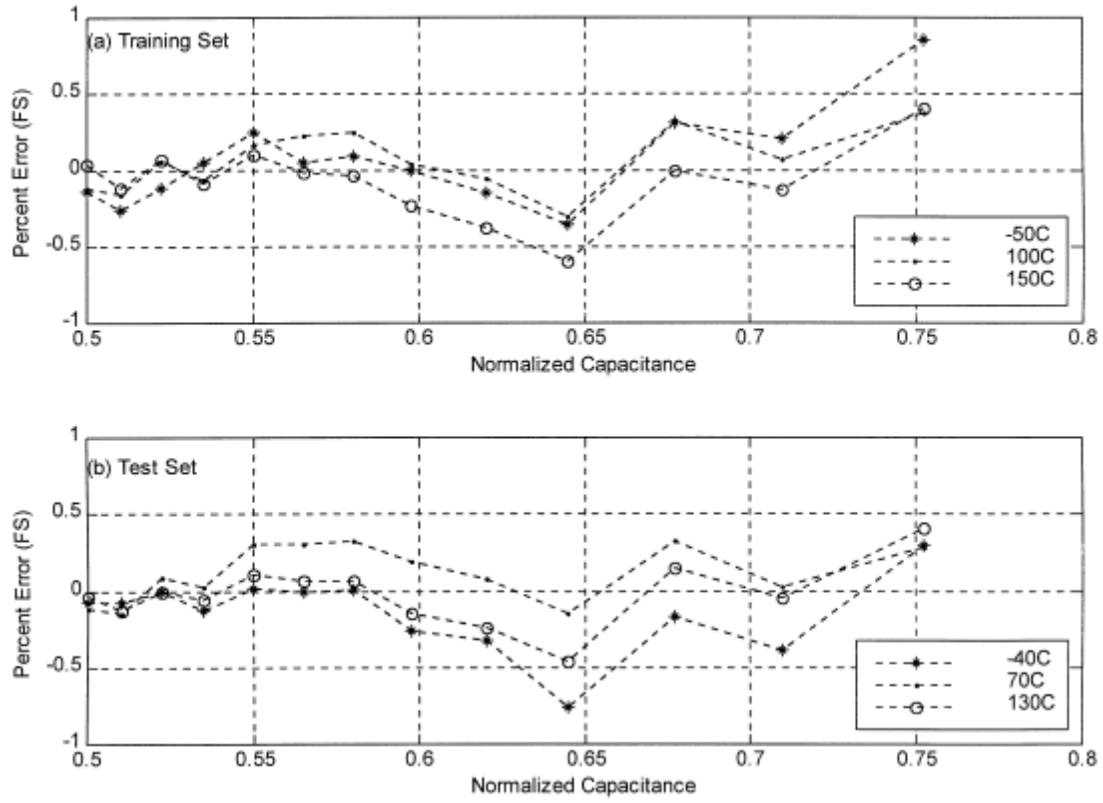


Fig. 9

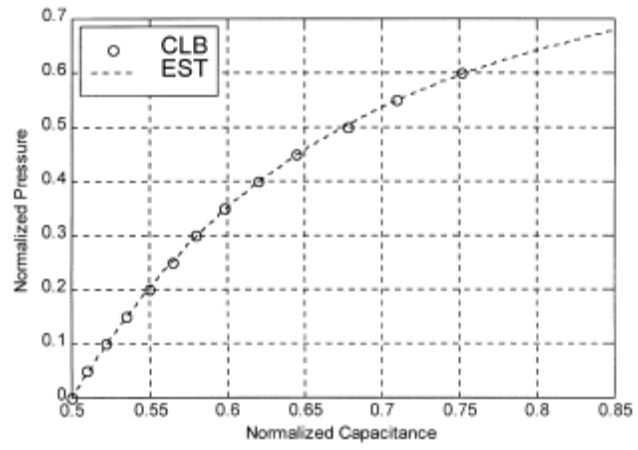


Fig. 10

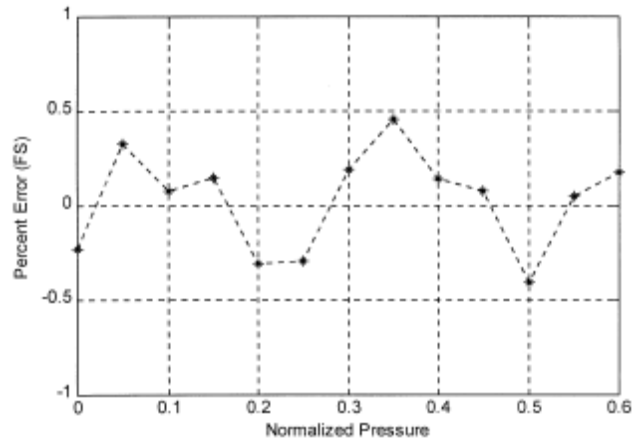


Fig. 11

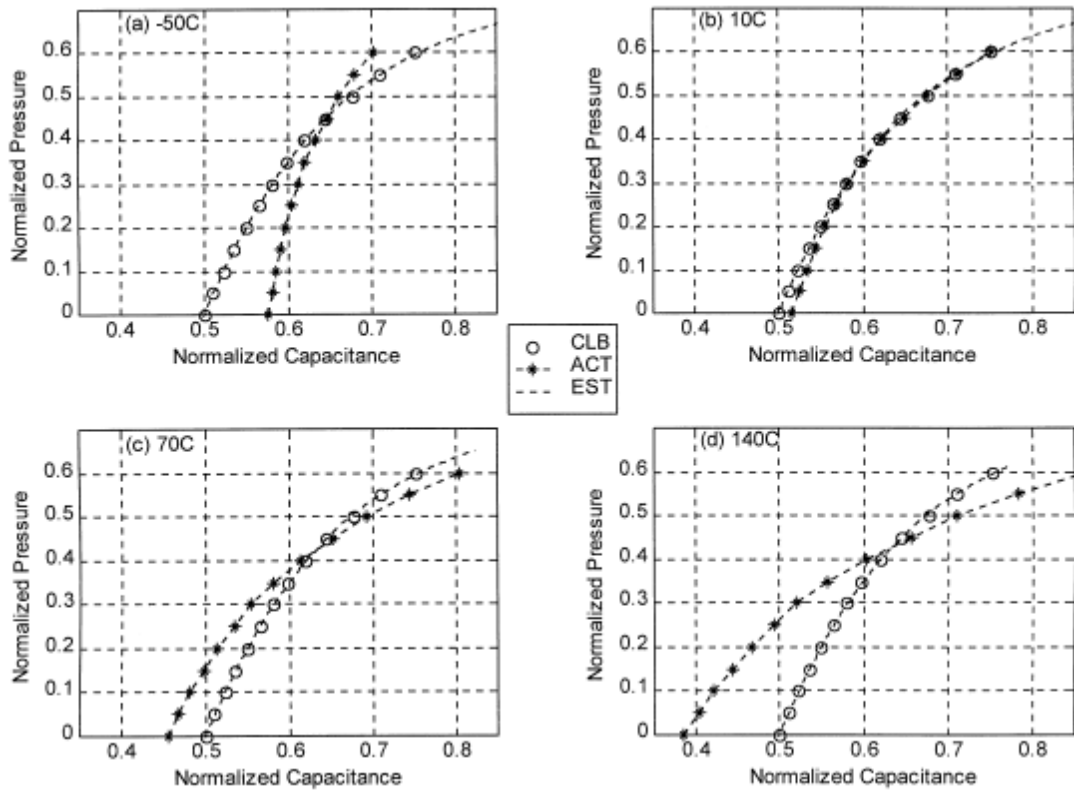


Fig. 12

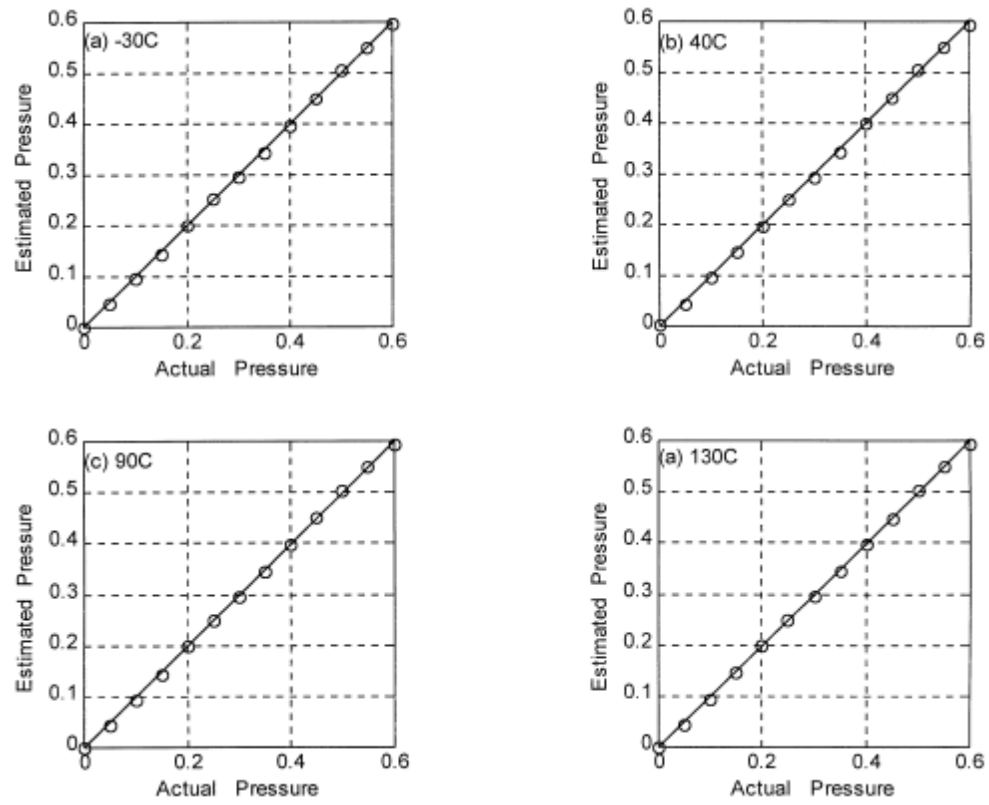


Fig. 13

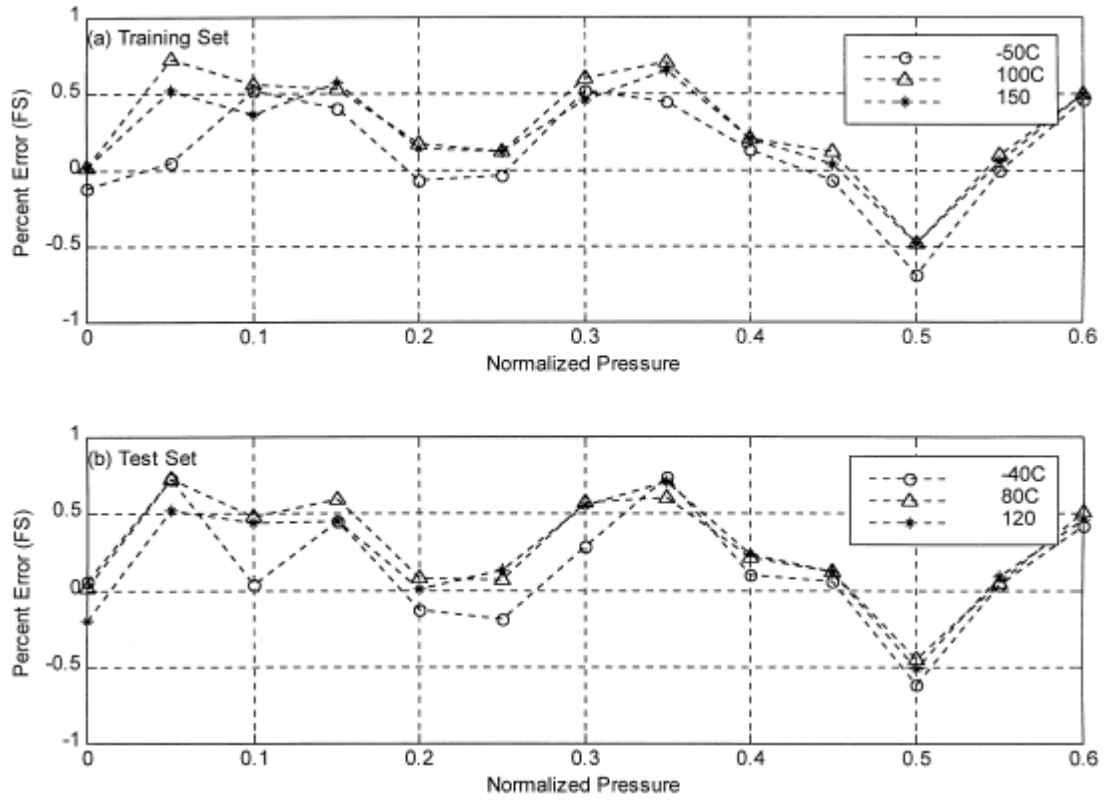


Fig. 14

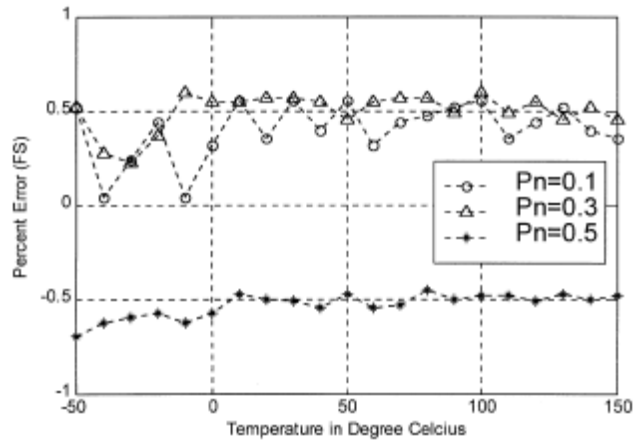


Fig. 15

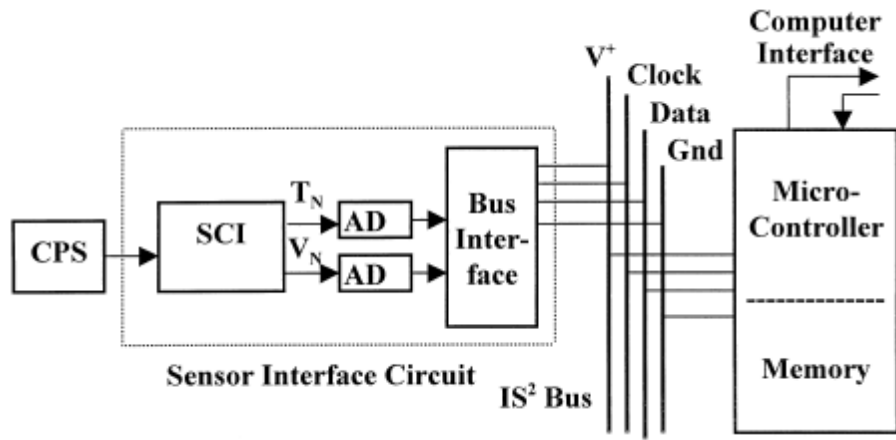


Fig. 16

## Biography



Jagdish Chandra Patra was born on January 15, 1957 in Nowrangpur, Orissa, India. He received B.Sc (Engg.) and M.Sc. (Engg.) degrees in Electronics & Telecommunication Engineering from Sambalpur University, Orissa in 1978 and 1989, respectively. He earned his Ph. D. degree from the Department of Electronics & Electrical Communication Engineering, Indian Institute of Technology, Kharagpur in 1996.

After obtaining Bachelor's degree, Dr. Patra served different teaching, research & development, and industrial organizations. In 1987, he joined as a lecturer in the Department of Electrical Engineering, Regional Engineering College, Rourkela, Orissa. In 1990, he was promoted to an Assistant Professor in the Department of Applied Electronics and Instrumentation Engineering of this College and till now he is continuing there.

Dr. Patra was a Guest Teacher (Gastdoscent) in the Department of Applied Physics, Delft University of Technology, The Netherlands, during April-October 1999. Now, he has joined the Nanyang Technological University, Singapore, as a Research Fellow by taking leave from his parent College.

Dr. Patra has published several research papers in national and international journals of repute. His research interest includes signal processing using intelligent techniques such as artificial neural networks, fuzzy logic and genetic algorithms. He is a member of IEEE (USA), Institution of Engineers (India) and a life member of Indian Society for Technical Education.



Adriaan van den Bos is a full professor of physics at Delft University of Technology, Delft, The Netherlands. At the same institute he was awarded the Physics Engineering degree and the Doctor of Technical Sciences degree in 1962 and 1974, respectively. Professor Van den Bos is author of more than 40 journal papers, one of which has become a Citation Classic. He is a Fellow of the IEEE.